Atomistic Simulations of Effect of Coulombic Interactions on Carrier Fluctuations in Doped Silicon

Zudian Qin and Scott T. Dunham
University of Washington, Department of Electrical Engineering, Seattle WA 98195, U.S.A.

ABSTRACT

Carrier distributions associated with point charges in silicon solved with quantum perturbation theory are used to determine Coulombic interactions between charged defects in the presence of carrier screening. The resulting interactions are used in kinetic lattice Monte Carlo (KLMC) simulations of point defect-mediated diffusion to study dopant redistribution and associated variations in carrier concentration. Over a broad range of doping concentrations and temperatures, Coulombic repulsion between like dopants leads to ordering, resulting in a more uniform electrical potential distribution and therefore reduced variations in device performance compared with random doping, the standard condition assumed in previous doping fluctuation analyses.

INTRODUCTION

Fluctuations in carrier density due to both dopant number and location variations have been identified as a critical issue in controlling device performance (e.g., threshold voltage V_{th} variations control) in nanoscale MOSFETs [1-3]. To date, analysis of this phenomenon has largely assumed that the dopants are distributed randomly within active regions [4-8]. However, interactions between dopants during device fabrication can lead to correlations in dopant locations, modifying the resulting variations. One source of such correlations is the Coulombic interactions between ionized dopants, screened by nearby free carriers. In this work, we examine the effect of these interactions on variations in electrical potential within doped regions via kinetic lattice Monte Carlo (KLMC) simulations [9-11], which simultaneously solve for free carrier distributions and include the effect of associated potential variations on the diffusion of charged dopants and point defects.

To study doping fluctuations, a tool must first be capable of tracking dopant locations within the system. Traditional continuum simulators lack such capability since they focus on macroscopic-level averages (e.g., dopant concentrations) within the system without giving any information on locations of individual atoms. Kinetic lattice Monte Carlo simulations, on the other hand, are well suited to this task. The KLMC simulations utilized in this work operate on a 3D silicon (diamond) lattice structure with impurities and point defects mapped to lattice sites [9-11]. The system evolves through transitions from one atomic configuration to the next, by virtue of point defect migration/reactions. The rates of these transitions are determined by the migration barriers combined with changes in system energy associated with transitions:

$$\nu = \nu_0 \exp\left(\frac{-E_m}{k_B T}\right)\exp\left(\frac{E_i - E_f}{2k_B T}\right) \quad (1)$$

where E_m is the unbiased migration barrier, E_i and E_f are the system energies before and after the transition, and T is the system temperature. The system energies are calculated based on the atomic arrangements of impurities/defects, with parameters from *ab-initio* calculations and/or experimental observations. At each simulation step, one transition is chosen from the possible set based on the relative rates, and the system time is advanced by the inverse of the sum of the rates. By only considering transitions (and not lattice vibrations) associated with defects and impurities present in the system, the KLMC method overcomes the time-scale limits associated with molecular dynamics to consider macroscopic system and processing time scales.

KLMC SIMULATIONS WITH COULOMBIC INTERACTIONS

In KLMC simulations Coulombic interactions between charged defects are modeled by Coulombic energy of the system. To obtain the Coulombic energy, we first compute the overall free carrier distribution based on charged defect locations inside the system, with a positively charged defect (e.g., an ionized donor) inducing an electron cloud in its neighborhood and a negatively charged defect (e.g., an ionized acceptor) inducing a hole cloud. The overall carrier distribution is the summation of contributions from all charged defects. The model for carrier distribution induced by a point charge was based on a solution to the Poisson equation by quantum perturbation theory [11]. The Columbic energy for use in the KLMC diffusion simulations is then calculated by:

$$E_{Coul} = \sum_i z_i \times \phi \tag{2}$$

where z_i is the charge carried by the ith defect in the system and ϕ represents the local electronic potential level derived from the carrier density at the location using Boltzmann equation,

$$\phi = \frac{k_B T}{q} \ln\left(\frac{n}{n_i}\right) \tag{3}$$

with n_i being the intrinsic carrier concentration.

To analyze the effect of Coulombic interactions on doping fluctuations, dopant atoms are first randomly initialized in the system. The initial carrier densities and associated potential distribution are evaluated at room temperature. The system is then annealed within the KLMC framework at an elevated temperature. After annealing, the potential distribution is reevaluated at room temperature. During the annealing process, the carrier and potential distributions are calculated for the annealing temperature after each simulation step to reflect the evolved system configuration with current locations of charged defects and/or ionized dopant atoms.

KLMC SIMULATION RESULTS

Fig. 1 compares histograms of the potential distribution within the system, one for the initial random doping and the other after annealing. Notice that the system has a narrower potential distribution after annealing. We attribute this to dopant/dopant repulsion leading to a more

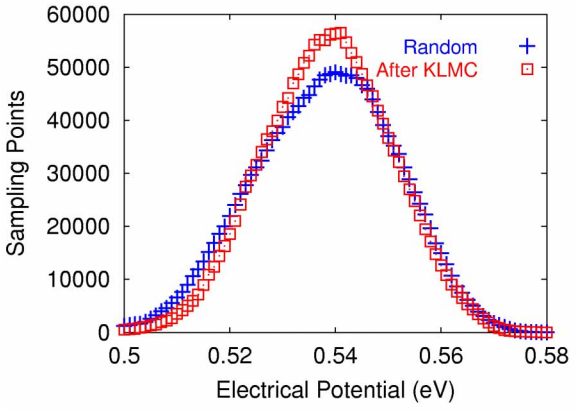

Figure 1. Histogram over lattice sites (2 million) of electrical potential before and after annealing at 1000°C. Annealing leads to narrower potential distribution, indicating effect of Coulombic interactions on dopant redistribution.

uniform dopant distribution (ordering). In confirmation, no narrowing in the potential distribution is observed if the effect of the potential on dopant diffusion is neglected.

The extent of potential variations within the system can be characterized in terms of its standard deviation. Fig. 2(a) and (b) demonstrate results from simulations on systems with various background doping annealed at 700°C and 1000°C for both *n*-type and *p*-type material. In all cases, we observed reduced standard deviation of potential distributions after annealing. As would be expected, narrower potential distributions are achieved for both lower temperature

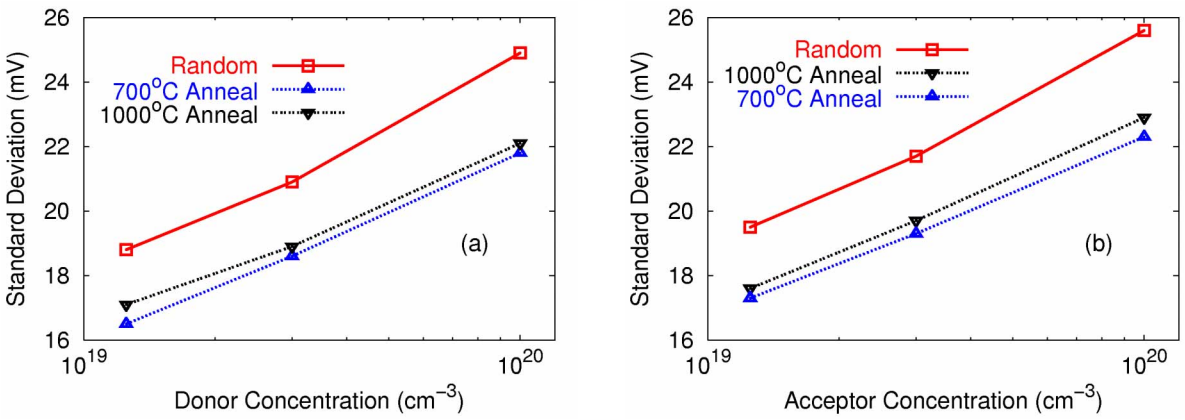

Figure 2. Standard deviation of electron potential versus concentrations for (a) donor and (b) acceptor doping before and after annealing at 700°C or 1000°C. In all cases, annealing shows a narrowed potential distribution attributed to Coulombic interactions between charged dopants. The distribution is broader for higher doping due to more sharply peaked carrier distribution screening dopants and for higher temperature due to stronger role of entropy. Differences between donor and acceptor doping arise from difference in conduction and valence band structure.

anneals and lower doping concentration systems. Lower temperatures lead to stronger ordering, as Coulombic repulsion is more effective compared to random hopping. Lower doping levels result in longer Debye lengths, so the potential varies less sharply around each dopant. Small differences are seen between *n*-type and *p*-type material, arising from the differences in density of states and effective mass. The conduction band having more extrema with larger curvature results in lower values of *k* for occupied states and thus weaker variations in carrier density.

DEVICE SIMULATIONS AND RESULTS

Device simulations were conducted to measure the impact of carrier fluctuations on device performance and in addition to assess the significance of dopant ordering caused by Coulombic interactions. The target device has an effective channel length of 18 nm in accordance with a projected MOS structure (45 nm node on ITRS) [12]. Each simulation device has a numerical channel doping either placed randomly or imported from an ordered system after KLMC anneal, with the average being 10^{19} cm^{-3}.

Fig. 3 plots drain current against gate voltage for a set of devices, which clearly shows variations in device performance. In Fig. 4, we compare threshold variations between devices with random doping and devices with ordered doping. The distribution profile for ordered systems is clearly more centered on its average, indicating reduced variations among samples. Fig. 5 compares variations in device performance based on extracted values of several device operation parameters, including threshold, sub-threshold slope, drain current at maximum gate voltage and maximum channel transconductance. As seen, annealing at both temperatures leads to reduced variations in all the parameters, with lower temperature (700°C) producing stronger effects. For instance, we observed a 45% reduction in threshold variations for devices annealed at 700°C compared to 26% for 1000°C anneal.

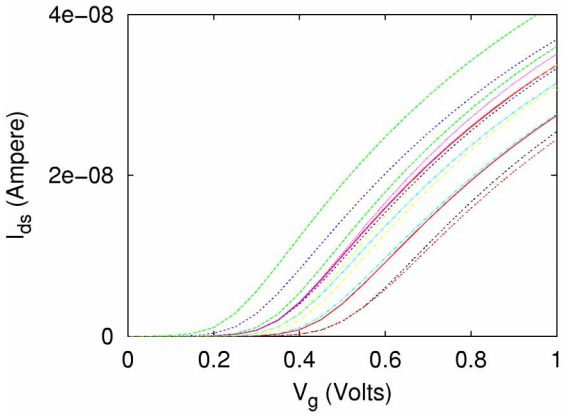

Figure 3. Device performance variations among samples shown on an I_{ds} vs. V_g plot.

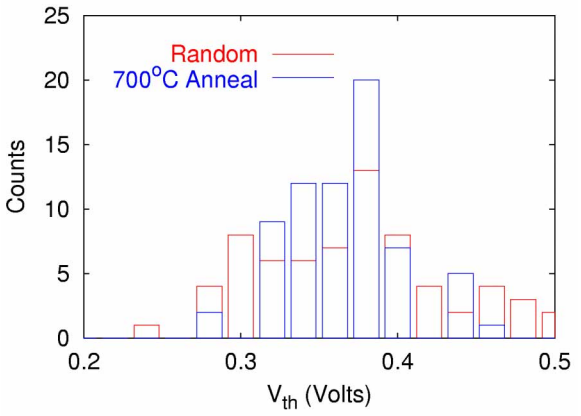

Figure 4. Comparison of threshold distribution between two groups of simulations, one with random channel doping and the other with ordered channel doping after anneal. A more restricted profile after anneal indicates a reduced variation in device performance.

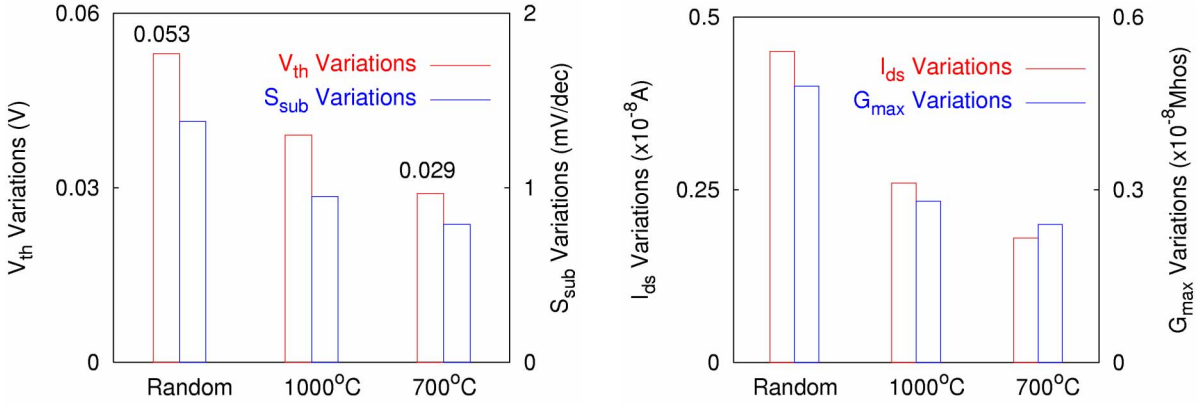

Figure 5. Comparison of device performance variations based on measurements of a few key parameters of device operation. The reductions in device performance variation are confirmed by all four measurements. Lower temperature annealing produced stronger dopant ordering and therefore greater reduction in standard deviation.

CONCLUSIONS

In conclusion, KLMC simulations based on a point charge-induced carrier distribution model have shown that Coulombic interactions between like dopants causes dopant ordering during annealing, resulting in a more uniform electrical potential distribution within the active region compared to standard approach with random dopant placement. This leads to reduced variations in device performance, enabling further device scaling. Lower temperature annealing gives rise to stronger ordering, producing even greater reduction in device parameter variations.

AKNOWLEDGEMENTS

This work was supported by the Semiconductor Research Cooperation (SRC). The device simulator (Taurus) was provided by Synopsys. Part of the calculations was conducted on a computing cluster donated by Intel. One of the authors, Zudian Qin would like to thank Mr. Chenluen Shih for his help on device simulations.

REFERENCES

1. B. Hoeneisen and C. A. Mead, *Solid-State Electron.* **15**, 819 (1972).
2. R. W. Keyes, *Proc. IEEE* **63**, 740 (1975).
3. T. Mizuno, J. Okamura, and A. Toriumi, *IEEE Trans. Electron Dev.* **41**, 2216 (1994).
4. A. Asenov, G. Slavcheva, A. R. Brown, J. H. Davies, and S. Saini, *IEEE Trans. Electron Dev.* **48**, 722 (2001).
5. N. Sano and M. Tomizawa, Appl. Phys. Lett. **79**, 2267 (2001).
6. I. D. Mayergoyz and P. Andrei, J. Appl. Phys. **90**, 3019 (2001).
7. Y. Yasuda, M. Takamiya, and T. Hiramoto, *IEEE Trans. Electron Dev.* **47**, 1838 (2000).
8. X. Tang, V. K. De, and J. D. Meindl, *IEEE Trans. VLSI Systems* **5**, 369 (1997).
9. S. T. Dunham and C. D. Wu, J. Appl. Phys. **78**, 2362 (1995).
10. M. M. Bunea and S. T. Dunham, in *Semiconductor Process and Device Performance Modeling*, *MRS Proc*. **490**, edited by S. T. Dunham and J. Nelson (Pittsburgh, 1998), p. 3-8.
11. Z. Qin and S. T. Dunham, *MRS Proc.* **717**, C3.8 (2002).
12. *International Technology Roadmap for Semiconductors* (ITRS): Executive Summary (2001), p. 38, Table 1f.